Available online at www.sciencedirect.com
SCIENCE DIRECT®
Journal of Power Sources xxx (2005) xxx–xxx
JOURNAL OF POWER SOURCES
www.elsevier.com/locate/jpowsour

Performance and ageing of an anode-supported SOFC operated in single-chamber conditions

X. Jacques-Bédard [a], T.W. Napporn [a,*], R. Roberge [b], M. Meunier [a]

[a] *Département de Génie Physique, École Polytechnique de Montréal, Montréal, Qc, Canada H3C 3A7*
[b] *Institut de Recherche d'Hydro-Québec, Varennes, Qc, Canada J3X 1S1*

Received 28 February 2005; received in revised form 17 March 2005; accepted 20 March 2005

Abstract

Anode-supported cells made of conventional materials were tested in single-chamber conditions under various CH_4/air gas mixtures. Methane-to-oxygen ratio (R_{MIX}) and nominal temperature between 600 and 800 °C both affect the performance of the cell. At a flow rate of 350 sccm, maximum values of power density (260 mW cm^{-2}) and cell voltage (1.05 V) were obtained for $R_{MIX} = 2$ at 800 °C. However, short term ageing experiments show that the stability of the cells depends on R_{MIX} as well as the flow of current. Scanning electron micrographs (SEM) reveal some important changes in anode microstructure close to the fuel inlet that may be, assign to the volatilization of the nickel contained in the Ni–YSZ cermet.

Keywords: Single-chamber SOFC; Anode-supported cell; Ni–YSZ cermet; Anode ageing

1. Introduction

Single-chamber solid oxide fuel cell (SC-SOFC), where both electrodes of a cell are exposed to a uniform mixture of fuel and air is an alternative approach to the more traditional fuel cell configuration, where the anode and the cathode components are placed in separate compartments. SC-SOFCs should lead to significant cost reduction of stack manufacturing by eliminating the sealing processes and simplifying the gas distribution over the individual electrodes. As for the more traditional high temperature cells, they may be exposed to various fuels [1,2]. In all cases, their working principle is based on the selectivity of the electrodes towards the fuel and the air. In methane–air mixture, for example, the anode should be active towards the partial oxidation of methane (Eq. (1)) as well as the electrochemical oxidation of CO (Eq. (2)) and H_2 (Eq. (3)) thus produced:

$$CH_4 + \tfrac{1}{2}O_2 \rightarrow CO + 2H_2 \quad (1)$$

$$CO + O^{2-} \rightarrow CO_2 + 2e^- \quad (2)$$

$$2H_2 + 2O^{2-} \rightarrow 2H_2O + 4e^- \quad (3)$$

Moreover, the cathode should favour the electrochemical reduction of oxygen (Eq. (4)).

$$O_2 + 4e^- \rightarrow 2O^{2-} \quad (4)$$

Oxygen consumption at the anode (Eqs. (2) and (3)) generates a gradient of the oxygen ion activity between the two electrodes which induces the build up of an electromotive force.

However, the electrochemical behavior of a methane–air mixture at elevated temperature is not as simple as the picture given above. Indeed, many other chemical reactions may occur between the chemical products and the reacting components of Eq. (1). Moreover, dynamic phenomena such as oscillatory reactions and temperature waves have been reported during the partial oxidation of methane for the production of

* Corresponding author. Tel.: +1 514 340 4711x4635; fax: +1 514 340 3218.
E-mail address: teko.napporn@polymtl.ca (T.W. Napporn).

0378-7753/$ – see front matter © 2005 Elsevier B.V. All rights reserved.
doi:10.1016/j.jpowsour.2005.03.138

synthetic gas (syngas) over nickel-containing catalysts [3,4]. Also, no agreement has been reached yet concerning the reaction pathway of the partial oxidation of methane, whether occurring in one step [5] or in sequential steps [6]. Suitable conditions of temperature, gas composition and flow rates should be determined that lead to high CO and H_2 selectivity on the anode side while avoiding carbon deposition reactions (Eqs. (5) and (6)) on the catalyst surface:

$$2CO \rightarrow C + CO_2 \quad (5)$$

$$CH_4 \rightarrow C + 2H_2 \quad (6)$$

Our previous works have shed some light onto the above-mentioned conditions [7,8]. For instance, materials used for current collectors, such as platinum, may exhibit a strong catalytic activity towards methane [7] and should be avoided for understanding the roles and effects of anode materials. Also, a precise evaluation of the true cell temperature is essential for measuring cell performance since overheating as high as 35 °C have been recorded resulting from the exothermic reactions involved in a methane–air mixture [8]. Moreover, some preliminary investigations have shown that state-of-the-art anode-supported cells made of conventional materials could provide good performance when operated in a single-chamber [8]. In double-compartment configuration, this type of cells provides high performance at reduced temperature for a range of fuels including hydrocarbons [9,10]. They are now receiving attention from several groups studying the single-chamber design [11–13]. Because of the complexity related to cell operation in a fuel–air mixture, many operating parameters remain to be clarified in order to reach optimal performance and stability. The fuel-to-oxygen ratio is one of those due to the numerous reactions involved in the single-chamber configuration. This is supported by the recent work of Stefan et al., who emphasize the strong influence of the gas composition on SC-SOFC performance [14]. In this work, the R_{MIX} ratio is systematically investigated and related to the anode-supported cell performance and ageing.

2. Experimental

Experiments were carried out in methane–air mixtures using anode-supported cells purchased from InDEC B.V. (batch #KS2A040126). They are made of conventional materials, i.e. a Ni/YSZ cermet as the anode, a 8YSZ electrolyte and a (La, Sr)MnO_3 cathode with layer thicknesses of about 600, 10 and 60 μm, respectively. Coupons of 7 mm × 7 mm were cut out from larger cells and tested in our experimental set-up, which as been described extensively in refs. [7,8]. Previous to cell operation, reduction of the cermet is carried out at a nominal temperature of 800 °C, a methane-to-oxygen ratio (R_{MIX}) equal to 2 and flow rate of 350 sccm. Testing was performed at nominal temperature between 800 and 600 °C, and at R_{MIX} ranging from 2 to 0.5. Polarization curves are recorded using an active current sink, and the voltage is monitored through reference wires exiting from the cell.

Due to the exothermic nature of the reactions involved between methane and air in the reactor, cell temperature may depart from its nominal value upon introduction of the gas mixture. A special attention is thus given in our experimental set-up to closely follow the actual cell temperature. As in our previous work [8], in addition to the thermocouple that controls the furnace temperature, a second thermocouple located just in front of the cell is used to monitor the exhausted gas temperature. This type K thermocouple is made of a fine gauge, 0.01 in. in diameter, supported by a thin alumina capillary. The hot junction is lightly coated with an Aremco 570S cement to prevent any catalytic effect with the reactive mixture. Cell temperature departing from their nominal value upon introduction of the gas mixture is recorded for various methane–air mixtures at 800 °C.

Scanning electron microscopy (SEM) (Hitachi model S-4200 equipped with a field emission gun) was used to observe the morphology of the electrodes. The chemical composition of the anode following cell exposition to the reactive mixture was determined by energy dispersive X-ray (EDX) microanalysis.

3. Results and discussion

The effect of the gas composition on the open circuit voltage, E_{OC}, is presented in Fig. 1. A maximum value of E_{OC} = 1.05 V is obtained in methane-rich mixture at 800 °C. A general tendency is observed at any furnace temperature in which E_{OC} gradually decreases as R_{MIX} is lowered. This trend is followed until a sudden drop occurs at R_{MIX} = 0.5 due to the cermet reoxidation. Between R_{MIX} equal 0.625 and 1.5, a slight increase of E_{OC} is also measured as the temperature is decreased from 800 to 600 °C. However, this tendency is not always met for methane-rich mixtures. At

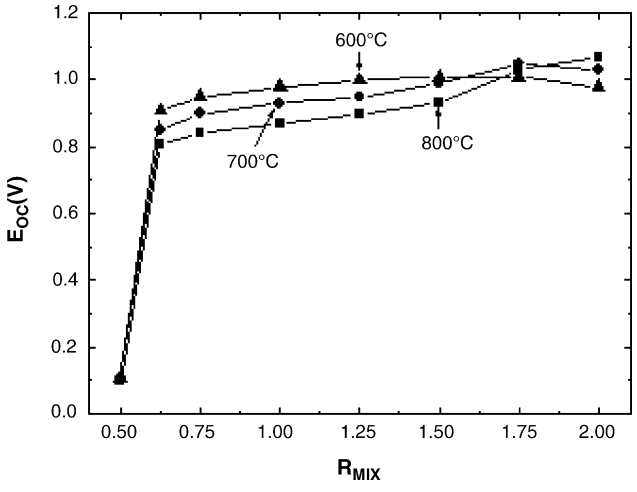

Fig. 1. Open circuit voltage E_{OC} as a function of R_{mix} at nominal temperatures T = 600, 700 and 800 °C and gas flow rate of 350 sccm.

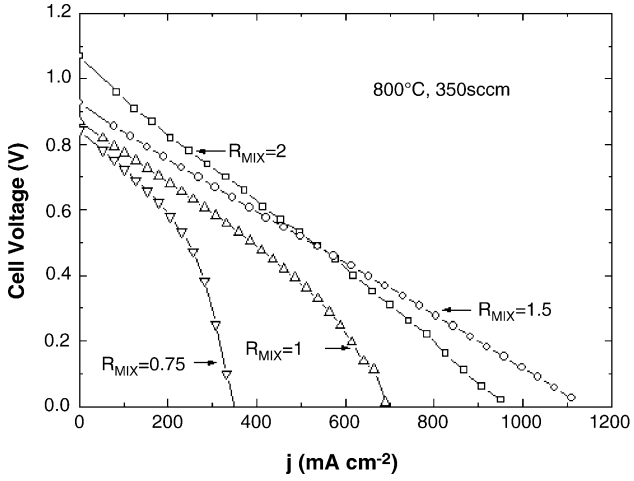

Fig. 2. *E–j* curves measured at a furnace temperature of 800 °C with a gas flow rate equal to 350 sccm for various R_{MIX}.

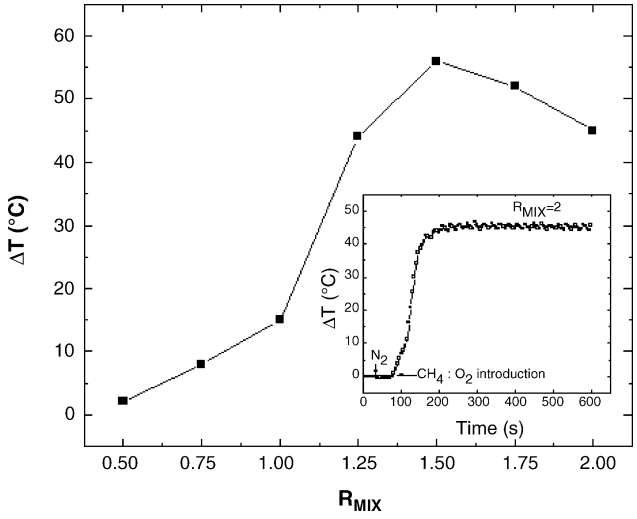

Fig. 3. Overheating of the outlet gas for various R_{MIX} under a gas flow rate equal to 350 sccm. Nominal temperature is 800 °C.

$R_{MIX} = 2$, for example, the order is reverse which may imply that carbon deposition is occurring at reduced temperature. This hypothesis is supported by the work of Zhan et al. [12] who studied propane–oxygen–argon mixture in slight excess of oxygen compared to the stoichiometric value expected from the partial oxidation reaction. Indeed, their thermodynamic calculations show that carbon deposition is starting to occur at 733 °C and that the amount of deposited carbon is rising until a constant level is attained at much lower temperature. Cell performances have been studied in various gas compositions. Voltage–current density (*E–j*) characteristics of the cells are shown in Fig. 2. Straight curves are observed at $R_{MIX} = 2$ and 1.5. However, decreasing R_{MIX} below 1.5, results in the appearance of diffusion-like phenomena at higher current densities. In oxygen-rich mixtures, this behaviour could be due to the higher formation of the total oxidation products H_2O and CO_2, which do not participate in the electrochemical reactions of the cell. We have recently confirmed this through real-time mass spectrometry measurements [15].

The comparison of the cell performance should take into account the true cell temperature, which may depart from its nominal value due to the exothermic reactions of the methane–air mixture. The actual cell temperature is strongly influenced by the gas composition as shown in Fig. 3. Our previous work has demonstrated that the heat evolved is related to the fuel oxidation reactions catalyzed by the Ni–YSZ cermet [7]. In Fig. 3, ΔT corresponds to the difference between the outlet gas temperature measured after full stabilization and the furnace temperature. The inset of Fig. 3 is an example of the outlet gas temperature variation after the gas mixture has been introduced into the reactor. Since the reading thermocouple is not in direct contact with the cell, the actual cell temperature may depart from that measured. However, these measurements are useful for comparing the heat evolved in various gas compositions. The highest exhausted gas overtemperature is measured in the range $1.5 \leq R_{MIX} \leq 2$. Thus, the better performance observed in methane-rich mixtures in Fig. 2 may also be assigned to a higher operating temperature. However, the overtemperature measurements of Fig. 3 are not in accordance with the higher potential heat of reaction available in oxygen-rich mixtures. As was observed before, mostly total reoxidation of the Ni cermet occurs at $R_{MIX} = 0.5$. From there and until a value of $R_{MIX} = 1.5$, similar arguments may be taken into account to suggest a decrease into the availability of the catalytic surface area. Moreover, Zhang et al. [3] reported that oxygen is competing with methane for adsorption sites on nickel surface and that excess oxygen has an inhibitory effect on the partial oxidation of methane. In our conditions, $R_{MIX} = 1.5$ corresponds to a threshold value below which the catalytic effect of the anode is hindered by the presence of excess oxygen.

The maximum power density P_{MAX}, measured from the discharge properties of the cells under the various gas compositions and furnace temperature examined here is represented in Fig. 4. For the whole range of temperature investigated, P_{MAX} is nearly constant for R_{MIX} comprised between 1.25 and 2. Values of about 260, 180 and 100 mW cm^{-2} have been obtained at the nominal temperature of 800, 700 and 600 °C, respectively. For $R_{MIX} = 2$ and $T = 800$ °C, the maximum power density of 260 mW cm^{-2} corresponds well to that obtained in our previous work [8]. However, the performance at R_{MIX} close to 1 is clearly lower than the 360 mW cm^{-2} obtained in similar conditions [8]. This may be explained by a different batch of cells used in the present study. The actual power densities are also less than the 280 and 210 mW cm^{-2} reported by Nammensma et al. [16] at 700 and 650 °C for InDEC cells operated in double-compartment under humidified hydrogen. However, their cells were exposed to a much higher flow rate of 700 sccm compared to the 350 sccm used here. Moreover, under single-chamber conditions, the fuel is not directly oxidized during the electrochemical processes, but

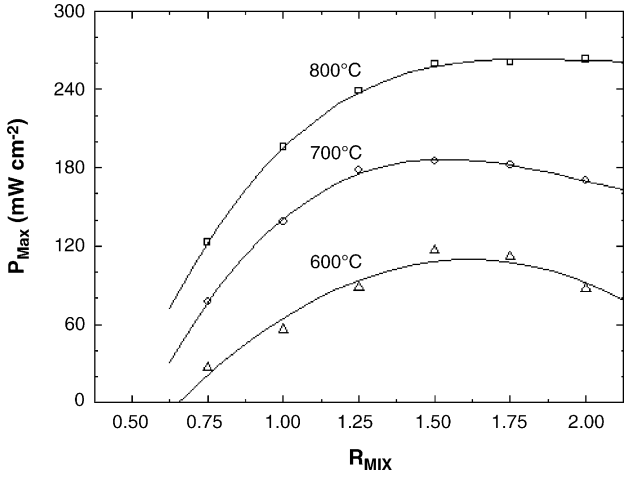

Fig. 4. Maximum power densities at various furnace temperatures and R_{MIX} under a flow rate of 350 sccm.

is rather generating the reacting H_2 and CO species through the partial oxidation of methane.

The open circuit cell voltage variations over a 72 h period under various gas compositions are illustrated in Fig. 5. The best stability is obtained at $R_{MIX} = 2$. It is, however, decreasing at $R_{MIX} = 1.5$ or 1 where stronger variations in the measured signals are observed. At the reduced time scale of Fig. 6, these variations of E_{OC} correspond to an oscillatory behaviour with a period of about 20 s at $R_{MIX} = 1$. Similar oscillations are observed for $R_{MIX} = 0.63$ in Fig. 5, whose period is more than 10 h. The oscillatory behaviour of E_{OC} could be due to oxidation and reduction cycles ongoing on the nickel surface, which proceeds at a speed that depends on the oxygen concentration of the gas mixture. These events may have an effect on the superficial heterogeneous reactions that involve the fuel oxidation. In order to better evaluate the effect of cell ageing, polarization curves have been measured before and after the test. As shown in Fig. 7, cell performance is nearly unchanged after 72 h exposure

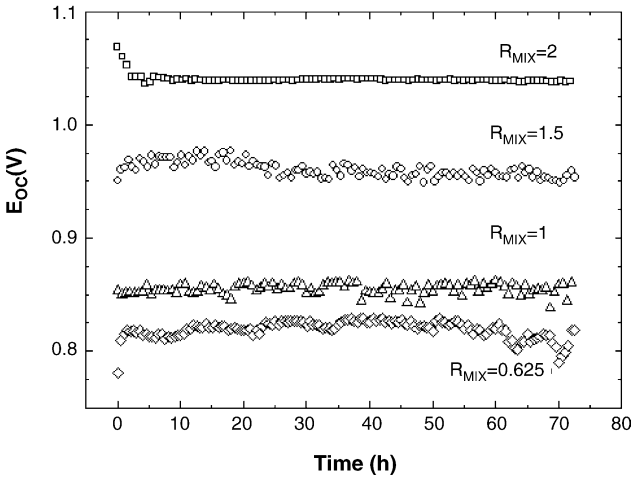

Fig. 5. Cell ageing at open circuit potential at furnace temperature of 800 °C at various R_{MIX} and under gas flow equal to 350 sccm.

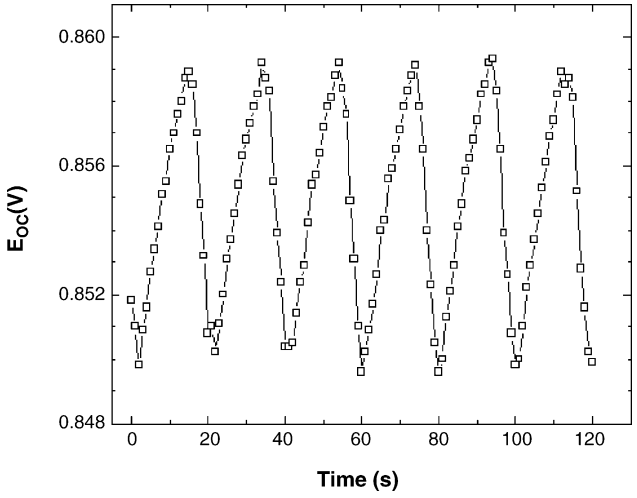

Fig. 6. Evolution of $E_{OC}(t)$ at reduced time scale after ageing for 72 h at $R_{MIX} = 1$.

at $R_{MIX} = 2$ in open circuit conditions. However, a clear degradation of the performance is observed after ageing at $R_{MIX} = 1$. Similar curves have been obtained for $R_{MIX} = 1.5$ and 0.63. Post-examination of the cells led to the observation of an extensive degradation of the anode near the fuel inlet for $R_{MIX} < 1.5$. In this region, a white stripe less than 0.5 mm wide was visible to the naked eye while the region near the fuel outlet remained unaffected and presented a metallic aspect. For the cell aged at $R_{MIX} = 1$, the microstructure of the anode observed by SEM near the electrolyte interface shows an increasing porosity close to the fuel inlet (Fig. 8a) in comparison to that near the fuel outlet (Fig. 8b). For the cell exposed to a $R_{MIX} = 2$ gas mixture, the microstructure is not affected by the test over the entire surface of the anode and closely resembles that of Fig. 8b along its whole length. In Fig. 9, the EDX spectra recorded along various positions of the anode–electrolyte interface for the cell exposed to a $R_{MIX} = 1$ gas mixture indicate a decrease of

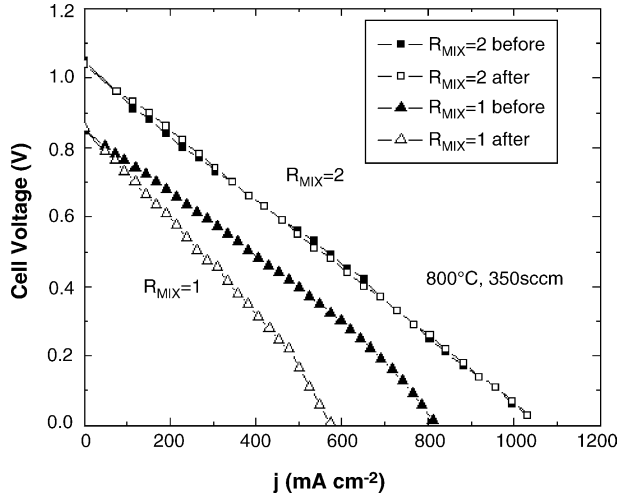

Fig. 7. Cells performances before and after ageing test at furnace temperature of 800 °C and 350 sccm.

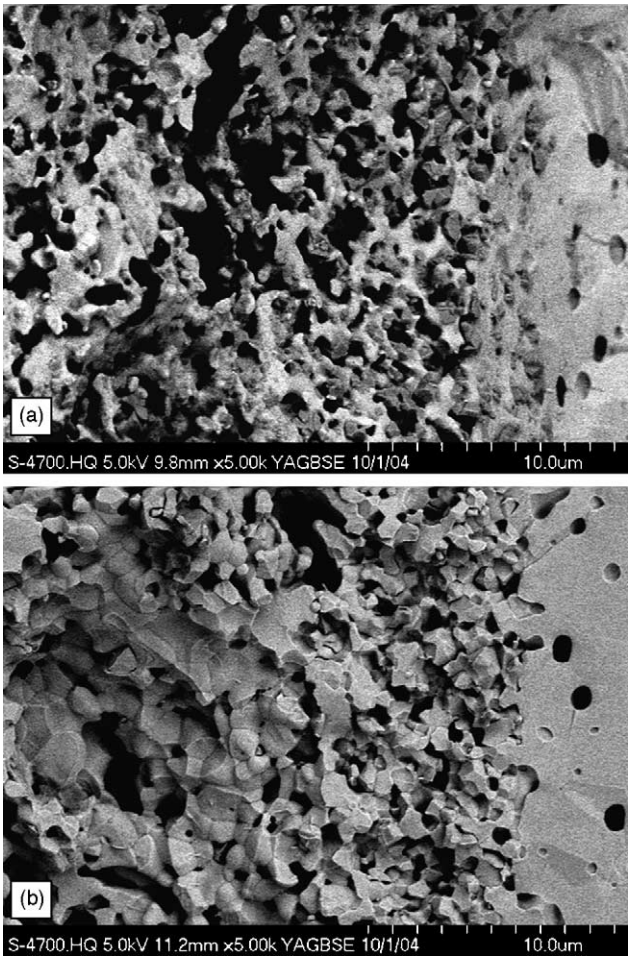

Fig. 8. Post mortem of anode-supported cell: cross section view of the anode–electrolyte interface near the fuel inlet (a) and fuel outlet (b) after 72 h ageing at furnace temperature of 800 °C, 350 sccm and $R_{MIX} = 1$.

the nickel concentration in the affected zone. The increasing porosity of the cermet where it is exposed to the incoming gas stream, could thus be explained by the reduce amount in Ni content and its further disappearance. This would leave the affected area with a whitening aspect that originates from an increase of the YSZ relative concentration. No such variation in the nickel signal was observed for the cell exposed to an $R_{MIX} = 2$ gas mixture. The degradation of the cell performance could thus be assign to a reduction of the anode active surface and electrical conductivity. Such a phenomenon have been reported by Torniainen et al. [17] who have noted a major reduction of the nickel content supported on foam monolith structure of Al_2O_3 and exposed to a methane–air mixture at a reaction temperature of 800 °C. After only 22 h test, the nickel concentration near the fuel inlet of their catalyst had dropped from 3 to 0.1%. However, no mechanism was provided to explain such nickel volatilization. Gubner et al. [18] have also put forward the high nickel reactivity at elevated temperature in the presence of methane gas and a high concentration of water vapour. Assuming that thermodynamic equilibrium is achieved in the

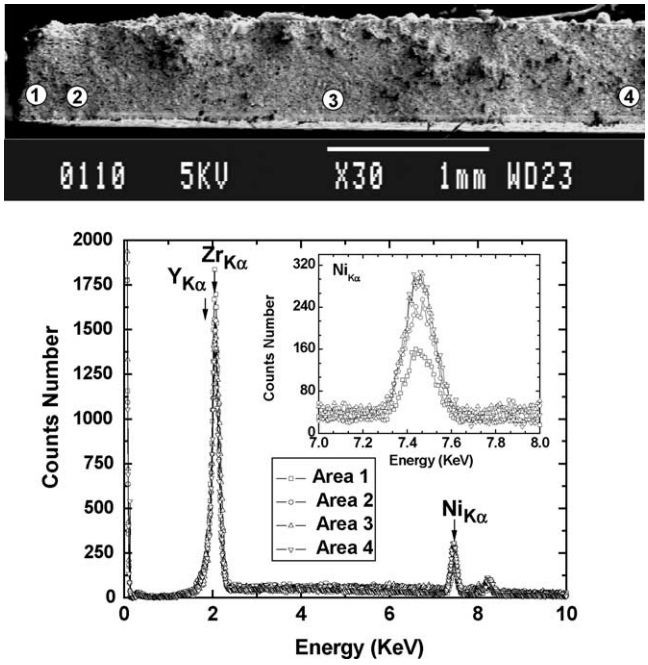

Fig. 9. EDX spectra measured along the anode–electrolyte interface after 72 h ageing at furnace temperature of 800 °C, 350 sccm and $R_{MIX} = 1$. The first spectrum has been recorded near the fuel inlet and the others at various positions towards the fuel outlet.

gas mixture, their calculations suggest that nickel hydroxide should exert a partial pressure close to 10^{-9} atm at 800 °C in a gas composition of 34% H_2 and 66% H_2O. In our case, the stream of incoming gas would flush away the $Ni(OH)_2$ thus formed and affects the cell performance over extended period of time. The reduction–oxidation cycles of the nickel surface that lead to the oscillations of E_{OC}, as discussed above, can also contribute to the degradation of the cell performance. Cassidy et al. [19], for instance, have shown that the volume change upon reoxidation of the nickel contained in the cermet anode was detrimental to their anode and supported thin electrolyte. For $R_{MIX} = 2$, oscillations in E were not observed and the cell was stable for at least 72 h. The phenomena of nickel volatilization and reduction–oxidation cycles could also explain the ageing of our electrolyte-supported cells [8].

Cell ageing has also been studied at 800 °C and $R_{MIX} = 2$ under various current loads. In Fig. 10, only slight degradation of performance is observed for currents of 330 and 800 mA cm^{-2}. However, at 535 mA cm^{-2}, where the maximum power density is found, rapid degradation is observed. Under such a condition, the terminal voltage starts to decrease after only 20 h of operation and leads to a 200 mV drop after 72 h. According to Appleby [20], the electrochemical oxidation of CO occurs more slowly than that of H_2 in high temperature fuel cells. The degradation of the performances could be related to carbon deposition favoured here by a high concentration of CO near the anode–electrolyte interface [21]. The better stability obtained at 800 mA cm^{-2} would be related to the high ionic flux of O^{2-} across the

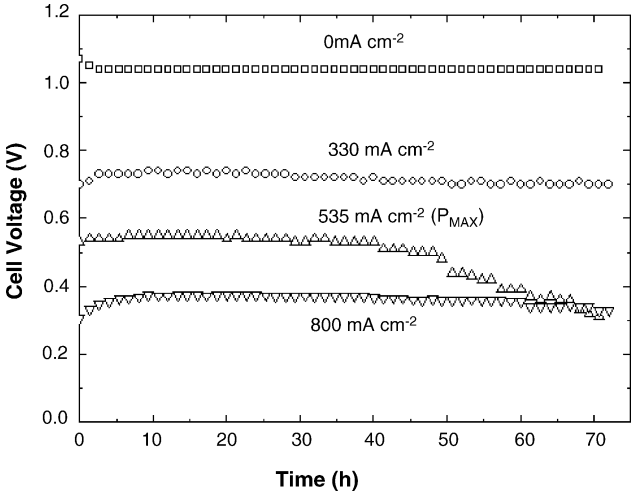

Fig. 10. Cell ageing at furnace temperature of 800 °C under various current densities. $R_{MIX} = 2$ and gas flow equal to 350 sccm.

electrolyte that favours the oxidation of the CO and prevents further carbon deposition [22].

4. Conclusion

In this study, anode-supported cells made of conventional materials have been shown to provide good performance when operated in a single-chamber design. Gas composition is a decisive parameter for the SC-SOFC that should be optimized in order to reach good cell performance and efficiency. The catalytic nature of cell operation plays a strong role in its overall behavior. For a Ni–YSZ/YSZ/LSM cell, a $R_{MIX} = 2$ gas mixture leads to better performance and stability under the temperature and flow rate conditions examined in this study. Under open circuit voltage, ageing processes that occur at $R_{MIX} < 2$ seem to be related to the nickel volatilization from the cermet. Moreover, an excess of oxygen gas, compared to the stoichiometric value expected from the partial oxidation reaction, results in the occurrence of some voltage oscillatory events induced by the reduction–oxidation cycles present at the nickel surface. This phenomenon is also contributing to the degradation of the cell. Under a specific range of flowing currents near the maximum power density, fast degradation may also occur probably due to carbon deposition processes. Further work is in progress to quantify the species found in the outlet stream of our single-chamber SOFC and evaluate the reaction pathways under characteristic operating conditions. Indeed, a better understanding of the catalytic aspect related to the partial oxidation of methane would be desirable as it is an essential part of the successful operation of the SC-SOFC.

Acknowledgements

The authors thank the Natural Sciences and Engineering Research Council of Canada and the Hydro-Québec for their financial support.

References

[1] T. Hibino, A. Hashimoto, T. Inoue, J.-I. Tokuno, S.-I. Yoshida, M. Sano, J. Electrochem. Soc. 147 (8) (2000) 2888.
[2] T. Hibino, A. Hashimoto, T. Inoue, J.-I. Tokuno, S.-I. Yoshida, M. Sano, J. Electrochem. Soc. 148 (6) (2001) A544.
[3] X. Zhang, D.O. Hayward, D.M.P. Mingos, Catal. Lett. 86 (4) (2003) 235.
[4] Y.P. Tulenin, M.Y. Sinev, V.V. Savkin, V.N. Korchak, Catal. Today 91–92 (2004) 155.
[5] V.R. Choudhary, A.M. Rajput, B. Prabhakar, A.S. Mamman, Fuel 77 (15) (1998) 1803.
[6] A.T. Ashcroft, A.K. Cheetham, J.S. Foord, M.L.H. Green, C.P. Grey, A.J. Murrell, P.D.F. Vernon, Nature 344 (1990) 319.
[7] T.W. Napporn, F. Morin, M. Meunier, Electrochem. Solid-State Lett. 7 (3) (2004) A60.
[8] T.W. Napporn, X. Jacques-Bédard, F. Morin, M. Meunier, J. Electrochem. Soc. 151 (12) (2004) A2088.
[9] A.V. Virkar, J. Chen, C.W. Tanner, J.-W. Kim, Solid State Ionics 131 (2000) 189.
[10] S. De Souza, S.J. Visco, L.C. De Jonghe, Solid State Ionics 98 (1997) 57.
[11] T. Suzuki, P. Jasinski, V. Petrovsky, H.U. Anderson, F. Dogan, J. Electrochem. Soc. 151 (9) (2004) A1473.
[12] Z. Zhan, J. Liu, S.A. Barnett, Appl. Catal. A 262 (2004) 255.
[13] A. Tomita, D. Hirabayashi, T. Hibino, M. Nagao, M. Sano, Electrochem. Solid-State Lett. 8 (1) (2005) A63.
[14] I.C. Stefan, C.P. Jacobson, S.J. Visco, L.C. De-Jonghe, Electrochem. Solid-State Lett. 7 (7) (2004) A198.
[15] T.W. Napporn, R. Roberge, S. Savoie, X. Jacques-Bédard, M. Meunier, Fuel Cells Science and Technology 2004, Scientific Advances in Fuel cell Systems, Munich, 6–7th October, 2004.
[16] P. Nammensma, J.P. Ouweltjes, G. van Druten, B. Rietveld, R. Huiberts, Fuel Cell Seminar 2002, Palm Springs CA, 18–21 November, 2002.
[17] P.M. Torniainen, X. Chu, L.D. Schmidt, J. Catal. 146 (1994) 1.
[18] A. Gubner, H. Landes, J. Metzger, H. Seeg, R. Stübner, SOFC V 97–18 (1994) 844.
[19] M. Cassidy, G. Lindsay, K. Kendall, J. Power Sources 61 (1996) 189.
[20] A.J. Appleby, J. Power Sources 49 (1994) 15.
[21] E.P. Murray, T. Tsai, S.A. Barnett, Nature 400 (1999) 649.
[22] C. Finnerty, N.J. Coe, R.H. Cunningham, R.M. Ormerod, Catal. Today 46 (1998) 137.